ChemCatChem

The European Society Journal for Catalysis

Chemistry Europe

European Chemical Societies Publishing

Supported by

GECATS GERMAN CATALYSIS SOCIETY

# Accepted Article

**Title:** Ru on Modified Carbon Submicrometric Spheres as Novel Catalysts for the Oxidative Cleavage of Oleic Acid with N-Methylmorpholine-N-Oxide as Green Oxidizing Agent

**Authors:** Sebastián Gámez, Ernesto de la Torre, and Eric M. Gaigneaux



**To be cited as:** *ChemCatChem* **2022**, e202201134

**Link to VoR:** https://doi.org/10.1002/cctc.202201134

WILEY-VCH

RESEARCH ARTICLE WILEY-VCH

# Ru on Modified Carbon Submicrometric Spheres as Novel Catalysts for the Oxidative Cleavage of Oleic Acid with N-Methylmorpholine-N-Oxide as Green Oxidizing Agent

Sebastián Gámez,*[a] Ernesto de la Torre[b] and Eric M. Gaigneaux[a]

[a] Professor Eric M. Gaigneaux and Sebastián Gámez
Institute of Condensed Matter and Nanosciences (IMCN)
Université catholique de Louvain
Place Louis Pasteur 1. L04.01.09, 1348 Louvain-la-Neuve, Belgium
E-mail: eric.gaigneaux@uclouvain.be, sebastian.gamez@uclouvain.be
Homepage: https://uclouvain.be/en/research-institutes/imcn/most/catalysis-and-chemistry-of-divided-materials-lab.html

[b] Professor Ernesto de la Torre
Department of Extractive Metallurgy
Escuela Politécnica Nacional
Ladron de Guevera E11-253, Quito 170517, Ecuador
Homepage: https://www.epn.edu.ec/departamento-de-metalurgia-extractiva-demex/

Supporting information for this article is given via a link at the end of the document.

**Abstract:** Oxidative cleavage of unsaturated fatty acids involves the rupture of carbon-carbon double bonds to produce carbonyl compounds of high added value. This reaction is mainly performed using homogenous catalysts which are pollutant and cannot be recovered while current heterogeneous catalysts display poor activity. To solve this issue, an active catalyst was prepared by impregnating Ru ions on carbon spheres synthesized by hydrothermal carbonization of a glucose solution. Carbon spheres were calcined under air atmosphere to create porosity and functionalized with polydopamine to improve their ability to complex Ru ions. The catalyst was fully characterized and completed the oxidative cleavage of oleic acid within 7 h of stirring at room temperature using $NaIO_4$ as oxidizing agent. The addition of N-Methylmorpholine N-oxide, a green oxidizing agent, allowed >99% conversion in only 5 h. Therefore, it was possible to conceive an eco-friendly carbon catalyst for the valorization of oleic acid under mild conditions.

## Introduction

Unsaturated fatty acids (UFAs) have become an interesting source of chemical base materials due to their abundance and low cost.[1-3] These molecules possess a carboxylic site and one or several unsaturations along their aliphatic chains.[4,5] Most of the reactions carried out on UFAs are focused on their carboxylic groups (e.g. decarboxylation, esterification, reduction) while around 10% of industrial applications are targeted to their unsaturations.[1,6,7] In this regard, the oxidative cleavage of carbon-carbon double bonds arises as an alternative for the production of value-added products from renewable feedstock.[8,9] For instance, oleic acid can be transformed into pelargonic (PA) and azelaic (AA) acids which are valuable as herbicides and skin cancer treatment respectively.[10,11] So far, oxidative cleavage of UFAs is mainly performed by ozonolysis (high energy demanding) or with homogenous catalysts which are not reusable and are polluting.[12-15] Moreover, current heterogeneous catalysts display a poor activity as a result of the poor contact amid the UFA and the active phase. In addition, bad performances of heterogeneous catalysts are related as well to loss of activity because of leaching issues.[16-18] In this matter we explored (i) the possibility to develop our own carbon supports and (ii) the modification of their textural properties by simple thermal treatments. To avoid polluting methodologies and to conceive a greener catalytic system, a hydrothermal eco-friendly carbonization procedure was selected to synthesize carbon submicrometric particles. This methodology uses different biomass derivatives (e.g. glucose, xylose, maltose, fructose, hydroxymethylfurfural) diluted in aqueous solutions which are heated under autogenous pressure inside sealed recipients.[19,20]

The most common and simple example is the hydrothermal carbonization of glucose which isomerizes into fructose during the autogenous heating process.[21-24] The latter decomposes into different organic derivatives such as levulinic acid, formic acid among others.[25-26] Fructose and glucose molecules may also undergo dehydration reactions followed by C-C bond breaking producing several soluble products like 1,6-anhydroglucose, erythrose, 5-hydroxy methylfurfural, or acetaldehyde.[27-29] The next stage of the hydrothermal carbonization process involves a polymerization of the previous intermediates via aldol condensation. These reactions produce a great amount of oligomers with different oxygenated groups.[30] Finally, an aromatization process takes place by means of intermolecular dehydration of the growing oligomers. During this step, various carbonyl groups (e.g. quinones, ketones, aldehydes) as well as C=C bonds arise due to the dehydration of hydroxyl groups along the monomer units.[30,31]

Next, a burst nucleation takes place when the concentration of aromatic oligomers in the aqueous solution attains the critical point of saturation. These nuclei grow outwards incorporating different species dissolved in the solution through stable oxygen bonds (i.e. ether or quinone bonds).[19,31] Throughout the whole carbonization process, these nuclei grow in the form of spheres with several aromatic layers increasing their particle size. When the heating stops, the outer surface of these carbon spheres exposes several oxygen groups (such as hydroxyls, aldehydes or carboxylic acids) while the inner layers possess less reactive

oxygenated species.[19,31] Hence, the particle size of these carbon spheres can be controlled by adjusting the hydrothermal carbonization time. Longer residence times lead to an extensive polymerization of the aromatic units which produces carbon spheres with bigger particle sizes.

Other parameters that influence the synthesis of carbon nanoparticles are the substrate concentration in the aqueous solution and the carbonization temperature.[32] The former is related to the yield of carbon spheres. The higher the concentration of the substrate in the aqueous solution, the higher the amount of produced carbon particles. As regards the carbonization temperature, it can also influence the size of carbon spheres. Higher carbonization temperatures contribute to extensive polymerization which leads to bigger carbon particles.[32,33] In order to modify the textural properties of these carbon particles, a calcination step under oxygen atmosphere can be applied. Joula and Farbod demonstrated that a post-calcination treatment at 350-420 °C can remove the outer layers of carbon particles through their combustion.[20] Then, the $CO_2$ generated during this combustion process can react with superficial carbon layers producing CO as well as porosity (which increases the specific surface area) in carbon nanoparticles.[34,35] Therefore, by combining a hydrothermal carbonization technique and a post-calcination treatment, it would be possible to easily synthesize nanoscale carbon particles with high surface area and a great amount of oxygen groups suitable for the complexation of metal cations.

Keeping the environment in mind, the possibility to replace $NaIO_4$ by a softer and greener oxidizing agent was explored in the oxidative cleavage of oleic acid. Although $NaIO_4$ is an efficient oxidizing agent in this reaction, it is also polluting for the environment. It has been reported that $NaIO_4$ is toxic for the aquatic life.[36,37] In this matter, amine oxides specifically N-methyl morpholine N-oxide (NMO), appear as greener alternatives. This organic compound is a heterocyclic amine oxide and morpholine derivative which is used in organic chemistry as a co-oxidant along with osmiates and perruthenates.[38,39] From the chemistry of osmium, it is known that NMO can give its oxygen atom to regenerate $H_2Os(VI)O_4$ into $Os(VIII)O_4$ during the dihydroxylation of olefins. The ability of NMO to oxidize this osmium species could also be used in the oxidation of Ru species during oxidative cleavage reactions.[39,40] Moreover, NMO is not bioaccumulative nor toxic for the aquatic life.[41]

Therefore, in this work we propose the synthesis of our own carbon supports by submitting a glucose aqueous solution to a hydrothermal carbonization under autogenous pressure to produce carbon particles. The latter will be calcined under air atmosphere to create porosity and therefore to increase the specific surface area. To enhance the support capability to form Ru complexes, polydopamine (PDA) will be added on calcined carbon particles surface (CCN). PDA is a polymer formed by indole ring units with amine and catechol groups suitable for Ru complexation. Thus, carbon particles with Ru (CN-Ru), CCN-Ru and CCN-PDA-Ru were assessed in the oxidative cleavage of oleic acid using $NaIO_4$ and NMO as oxidizing agents.

## Results and Discussion

### Characterization results

TEM images displayed in Figure 1 demonstrate that the hydrothermal carbonization method produced very regular carbon spheres with a mean diameter of 336 nm. After the calcination treatment, the mean particle size of CNs decreased down to 221 nm confirming that combustion of CNs outer layers led to smaller carbon particles. As onion layers, the external films of CNs are removed during the calcination process under air. On the other hand, when PDA was added to calcined carbon particles (CCNs), the mean particle size increased by about 20 nm. Figure 1e shows a layer of polymer that glues the carbon spheres confirming the adherence capability of this polymer on carbon materials.

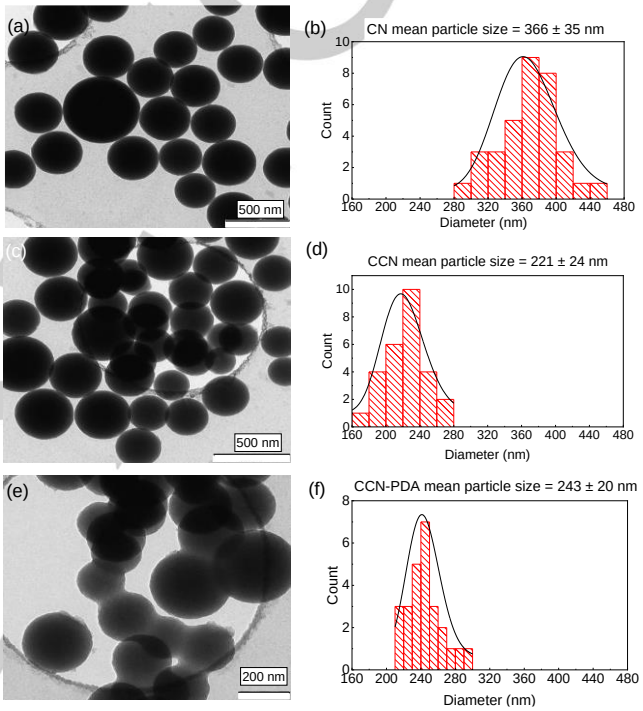


**Figure 1.** a) TEM image and b) particle size distribution of carbon particles (CNs); c) TEM image and d) particle size distribution of calcined carbon particles (CCNs) and e) TEM image and f) particle size distribution of CCN-PDA.

As regards the textural properties obtained through $N_2$ physisorption tests, CNs displays a type II isotherm which is characteristic of macroporous/non porous materials (Figure 2a). As a consequence, CNs present a low surface area as well as a low pore volume (Table 1). The means pore size (~25 nm) should be understood as the spaces between carbon spheres. On the contrary, CCNs display a type I isotherm which is assigned to microporous materials. Moreover, the specific surface area increased greatly (668 $m^2/g$) with respect to carbon particles without calcination. The $CO_2$ generated after the combustion of the outer layers on CNs surface can react with external carbon atoms that remained after the combustion.[19,42]

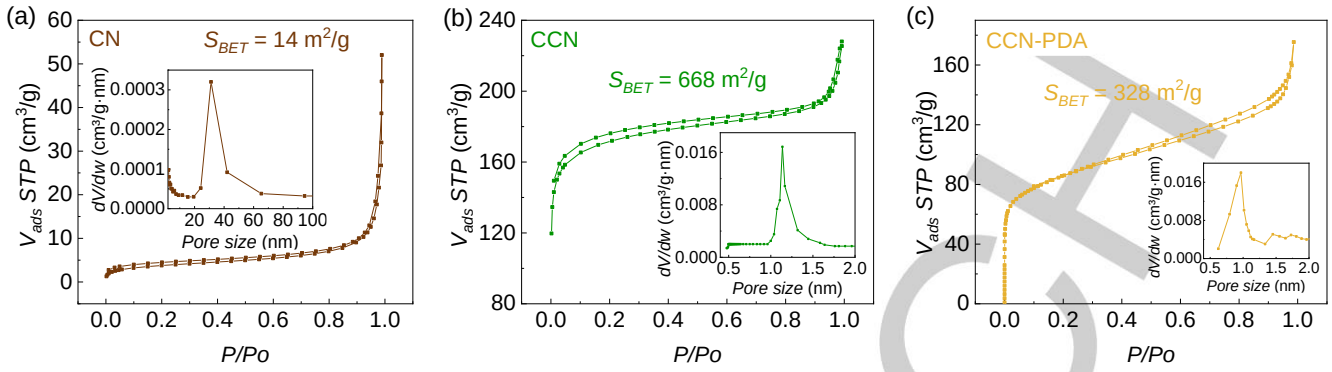


**Figure 2.** $N_2$ adsorption-desorption isotherms and pore size distribution of: a) CN; b) CCN and c) CCN-PDA.

In consequence, CO is generated while oxygen atoms can be incorporated on the carbonaceous matrix yielding surface oxygenated complexes represented by C(O) as follows:

$$C_{(s)} + CO_{2(g)} \rightarrow CO_g + C(O)_{(s)} \quad \text{[Eq. 1]}$$

Then the adsorbed oxygen C(O) may evolve into C-O bonds or they can be gasified in the form of CO.[43] Therefore, the most reactive and disorganized carbons are gasified generating spaces in the carbon matrix. Thus, the loss of carbon atoms due to this gasification creates porosity in the treated material.[42,43]

**Table 1.** Textural properties of carbon particles.

| Carbon Material | Specific surface area ($m^2$/g) | External surface area ($m^2$/g) | Pore Volume ($cm^3$/g) | Mean Pore size (nm) |
|---|---|---|---|---|
| CN | 14 | 12 | 0.03 | 24.9[a] |
| CCN | 668 | 37 | 0.33 | 1.2[b] |
| CCN-PDA | 328 | 38 | 0.25 | 1.1[b] |

[a] Barrett-Joyner-Halenda method. [b] Horvath-Kawazoe method

This asseveration was confirmed after estimating the mean pore size of CCNs. The pore size distribution of CCNs displayed mostly micropores (1.0-1.5 nm) which could be an impediment for oleic acid diffusion due to its similar lengths (Figure S1). These micropores are smaller than the gaps between carbon spheres observed during TEM microscopy which confirm that $CO_2$ created ruptures in the carbonaceous matrix through carbon gasification (i.e. creation of porosity). The most important fact of the calcination process is related to the increase of external surface area which is the real surface that can be exploited for the deposition of PDA and the further impregnation of Ru. As is shown in Table 1, the external surface area of CCNs increased by a factor of 3 with respect to CNs.

Finally, PDA deposition on CCNs decreased their specific surface area as a consequence of micropores blocking. Polymer layers covered the surface of carbon nanoparticles filling the spaces between particles as well as blocking most of their micropores created after calcination. It is important to note that despite this event, the external specific surface area was maintained, preserving the benefit of CCNs on CNs. It is important to mention that after Ru impregnation; no significant changes were observed on the textural properties of the three carbon supports.

About the chemical properties of the synthesized carbon materials, Figure 3 shows the main functional groups determined by FTIR spectroscopy. Carbon particles shows a broad peak at 3426 $cm^{-1}$ which is assigned to the stretching vibration of hydroxyl groups. Two more peaks at 1726 $cm^{-1}$ and 1612 $cm^{-1}$ were also detected. The former is ascribed to carbonyl groups on CNs surface while the latter is characteristic of aromatic compounds.[44] Finally, a broad peak at 1220 $cm^{-1}$ is also detected and can be attributed to stretching vibrations in ethers.[44] These findings agree with the dehydration and aromatization processes ongoing during the hydrothermal carbonization.

The same characteristic peaks were also observed in the CCNs infrared spectrum. The presence of hydroxyl and carbonyl groups on CCNs confirms the fact that oxygen atoms can be incorporated on carbon particles during the calcination treatment. On the other hand, PDA deposition contributed with three additional peaks along a decrease in intensity of the band associated to carbonyl species (1726 $cm^{-1}$). Two bands at 1505 and 1435 $cm^{-1}$ are ascribed to stretching vibration modes from N-H in the indole ring and O-H in aromatic rings respectively.[45] The peak at 1268 $cm^{-1}$ is related to the stretching vibration of C-N bond in the same indole ring of PDA units.[45,46] Hence, these spectroscopic findings confirm the deposition of the polymer on CCNs surface. Moreover, there were not new peaks during FTIR analyses when CN-Ru, CCN-Ru and CCN-PDA-Ru were analyzed.

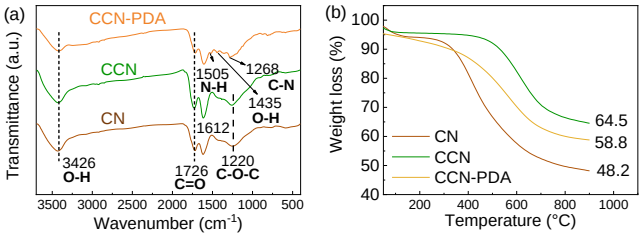


**Figure 3.** a) FTIR spectra of CN, CCN and CCN-PDA; b) TGA of CN, CCN and CCN-PDA.

Boehm's titration results summarized in Table 2 confirm the findings in FTIR spectra. CNs showed the highest total acidity of all carbon materials employed in this research work.

**Table 2.** Boehm's titration results of carbon particles.

| Carbon material | Phenols (mmol/g) | Lactones (mmol/g) | Carboxylic acids (mmol/g) | Total Acidity (mmol/g) |
|---|---|---|---|---|
| CN | 1.30 | 0.80 | 1.05 | 3.15 |
| CCN | 0.88 | 0.67 | 0.83 | 2.38 |
| CCN-PDA | 1.23 | 0.05 | 0.24 | 1.52 |

This outcome is due to the presence of oxygenated groups on carbon particles surface generated during the hydrothermal carbonization. Therefore, this green and simple method allowed to produce a carbon material with a great number of oxygenated groups suitable for transition metals complexation without using hazardous reagents which are detrimental for the environment. On the contrary, calcination treatment diminished the total acidity of carbon nanoparticles due to the gasification of carbon implying the elimination of oxygenated functional groups. After the deposition of PDA, the amount of hydroxyl groups increased because of the extra catechol groups provided by the polymer.

It is worth to mention that the presence of oxygenated groups on carbon surface will not be detrimental for PDA deposition but at the same time these functional groups may provide another way to interact with the polymer. Actually, PDA chains can interact with a carbon support by means of hydrogen bonds, π-stacking interactions or covalent bonds through Michael addition. Therefore, because of the different ways by which PDA can interact with several supports, the polymer chains will be deposited on a carbon surface regardless it possesses oxygenated groups or not.

On the other hand, oxygenated groups are essential for Ru complexation. Previous tests were performed with activated carbon and carbon black as supports to impregnate this transition metal by wet impregnation method. ICP analyses demonstrated that Ru complexation was not efficient to develop a catalyst with a Ru loading of 2 wt% and therefore, both carbon supports were functionalized to enhance their capability to complex Ru ions during the impregnation method. Oxidation treatment with $HNO_3$ was applied to both carbon supports and both of them with a higher amount of oxygen groups were able to complex Ru ions. In the present case, CN and CCN possess a high amount of oxygenated groups (Table 2), so forming complexes with Ru was not a problem. However, one must keep in mind that the calcination process contributed to the gasification of carbon along with several oxygenated functional groups. In fact, the hydrothermal carbonization method was responsible to generate all functionalities on carbon spheres surfaces. These asseverations were demonstrated by Boehm's titration on Table 2.

Thermogravimetric analyses displayed in Figure 3b indicated that the thermal stability of carbon particles increased after the calcination treatment. Most likely, tar and unpolymerized moieties produced after the hydrothermal carbonization were eliminated by combustion during the calcination treatment. In addition, by subtracting the weight loss of CCN-PDA from the weight loss of CCN, it was possible to estimate that about 6% of polydopamine was deposited on CCN surface. According to the values presented in Table S1, around 56% of the dopamine incorporated in the deposition was polymerized.

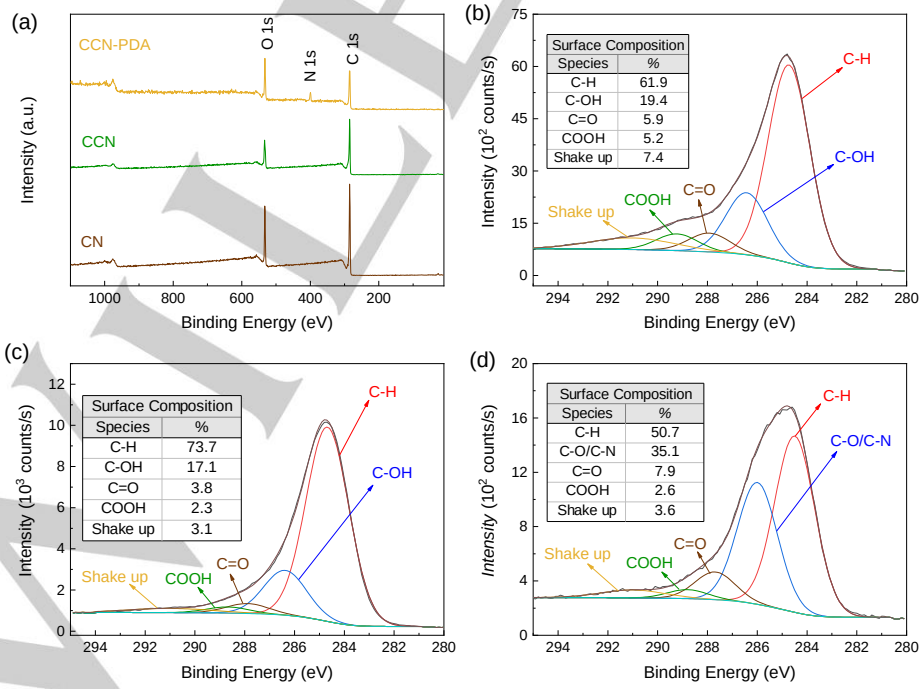


**Figure 4.** a) XPS survey spectra of CN, CCN and CCN-PDA; C 1s high resolution spectrum of b) CN, c) CCN and d) CCN-PDA.

PDA layers can interact with CCNs functional groups or with their aromatic layers by π-stacking interactions. XPS survey spectra displayed in Figure 4a show the main characteristic peaks at 284.8 and 532 eV which correspond to C 1s and O 1s respectively. As regards CCN-PDA, it is possible to observe a small contribution at 399 eV assigned to N 1s peak. The presence of the latter in the CCN-PDA XPS spectrum is attributed to nitrogen atoms within the indole ring of polydopamine which is deposited on CCN surface.

The deconvolution of the C 1s peak of carbon particles displayed in Figure 4b was performed assuming 5 contributions. The main sub-peak at 284.8 eV is attributed to aromatic carbons on the graphene layers and carbon contamination while the contribution at 286.4 eV is assigned to carbon bonded to hydroxyl groups. Three sub peaks at 287.6, 288.9 and 291.3 eV were also estimated which are ascribed to carbonyl compounds (C=O), carboxylic acids (COOH) and the shake-up peak typical of aromatic structures respectively. The same carbon species were detected in the C 1s high resolution spectrum of CCNs (Figure 4c); however, the amount of oxygenated groups was lower than the that found for CNs. These findings agree with Boehm's titration results and with the explanation provided by literature (i.e. losses of carbon and oxygenated groups are caused by carbon gasification during the calcination treatment).

The deposition of PDA on CCN surface broadens the C 1s peak displayed in Figure 4d. The contribution at 286 eV is attributed to catechol groups and/or C-N bonds from secondary amines within the indole ring of the polymer. This contribution was greater than carbonyl compounds or carboxylic acids confirming that the deposition of PDA provided supplementary catechol groups on CCNs surface. This contribution was also evidenced in the elemental surface composition recapitulated in Table S2 where the oxygen/carbon ratio increased from 0.29 (CCNs) to 0.48 (CCN-PDA). To sum up, PDA provided suitable functional groups for Ru complexation.

This assumption was verified by measuring the amount of Ru incorporated on the abovementioned carbon materials by ICP-AES spectrophotometry analyses. Indeed, Table 3 shows that Ru nominal value matched with ICP values confirming that functional groups of CN, CCN and CCN-PDA managed to chelate Ru ions from the aqueous medium during the wet impregnation process. On the other hand, Ru surface concentration obtained by XPS spectroscopy was higher than the nominal value because all the transition metal is distributed on the surface of each carbon support.

**Table 3.** Ru loading on carbon catalysts.

| Catalyst | Nominal Ru (wt%)[a] | Superficial Ru (wt%)[b] | Ru loading (wt%)[c] |
|---|---|---|---|
| CN-Ru(2%) | 2.0 | 10.4 | 1.7 |
| CCN-Ru(2%) | 2.0 | 11.0 | 1.8 |
| CCN-PDA-Ru(2%) | 2.0 | 2.5 | 1.8 |

[a] Nominal composition corresponding to 2 wt%. [b] Ru superficial content determined by XPS. [c] Ru loading determined by ICP-AES.

As regards Ru oxidation state on CCN-PDA surface, the deconvolution of the O 1s peak from CCN-PDA-Ru(2%) in Figure 5a shows a contribution at 528.9 eV which is attributed to Ru-O bonds. The same contribution was also observed in the cases of CN-Ru(2%) and CCN-Ru(2%) shown in Figures S3a and S3b respectively. On the other hand, the Ru 3p core level of CCN-PDA-Ru(2%) presented a doublet at 463.3 and 485.5 eV which corresponds to an oxidation state of Ru(III) (Figure 5b). Since no Cl 2p was detected during the XPS analyses, it is proposed that the transition metal is forming a Ru(III)-catecholate complex with catechol groups of PDA on calcined carbon nanoparticles surface.

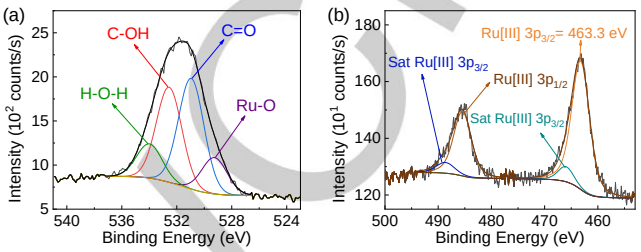


**Figure 5.** a) O 1s high resolution spectrum of CCN-PDA-Ru(2%); b) Ru 3p high resolution spectrum of CCN-PDA-Ru(2%).

### Catalytic tests

First, tests were performed by putting in contact oleic acid with the functionalized carbon supports in the solvent mixture without $NaIO_4$. The idea was to determine if oleic acid can be adsorbed on the surface of these carbon materials (i.e. to prove if oxygenated groups of carbon spheres may interact with oleic acid). In all cases no adsorption of oleic acid was detected demonstrating that oxygen groups of carbon supports do not interact with the substrate during the reaction.

The synthesized carbon catalysts were assessed in the oxidative cleavage of oleic acid using 8 equivalents of sodium periodate as oxidizing agent. Figure 6a shows that CCN-Ru(2%) displayed a greater catalytic activity than CNs. This fact is important because in our previous work it was demonstrated that the oxidative cleavage reaction with Ru-carbon black catalysts took place mostly in the reaction medium.[47] Thus, it would not matter what type of support was used for this reaction since the catalytic activity should have been the same. However, in this case, it was observed that CN-Ru(2%) (the catalyst with the lowest specific surface area) has the lowest conversion requiring 24 h to complete the reaction. On the other hand, the catalyst with a higher specific surface area completes the oxidative cleavage reaction in only 7 hours. This allows to conclude that the textural properties of the support (mostly the external surface area and pore size distribution) play a role in the oxidative cleavage of large UFAs such as oleic acid. Moreover, the addition of PDA on CCNs was not detrimental for the performance of the functionalize catalyst. Actually, CCN-PDA-Ru(2%) completed the oxidative cleavage of oleic acid after 7 h of agitation as well.

The same trend was also observed in the production of pelargonic (PA) and azelaic (AA) acids. Figure 6b demonstrates that yields and selectivities towards both desired oxidative cleavage products are improved when a carbon support with higher surface area than CNs is employed. It is important to remind that oleic acid evolves into PA and AA through different intermediates during the oxidative cleavage reaction.

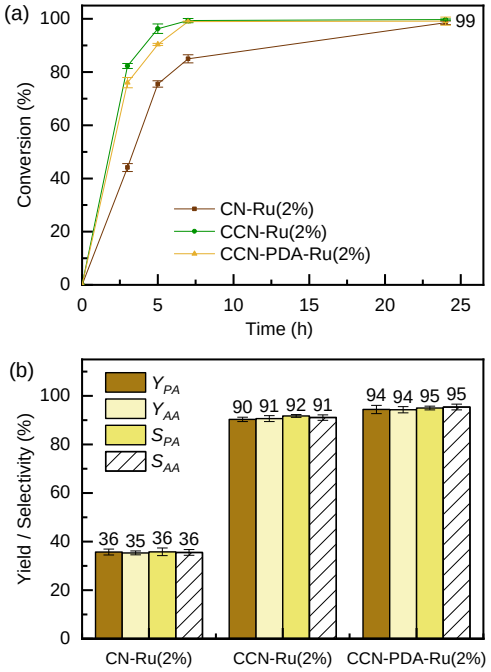


**Figure 6.** a) Catalytic activity of CN-Ru(2%), CCN-Ru(2%) and CCN-Ru(2%) in the oxidative cleavage of oleic acid with 8 equiv. of $NaIO_4$; b) Yields and selectivity towards pelargonic (PA) and azelaic acid (AA) achieved with carbon catalysts.

Briefly, oleic acid is transformed into 9,10 dihydroxystearic acid which is cleaved into nonanal and 9-oxononanoic acid. Both intermediates are over-oxidized into PA and AA by means of the oxidizing agent or by $Ru(VIII)O_4$.[47] These intermediates were still present after 24 h of stirring when CN-Ru(2%) was employed as catalyst (Figure S4). This was not the case when CCN-Ru(2%) or CCN-PDA-Ru(2%) were used in the catalytic tests suggesting that the textural properties of the carbon support may also intervene in the transformation of oleic acid into the desired carboxylic acid products.

The latter asseveration was also confirmed when CCN-Ru(2%) was compared with activated carbon (surface area = 1000 $m^2/g$) impregnated with the same Ru loading (i.e. 2 wt%). The as denoted ACO-Ru(2%) catalyst with a large surface area and extended microporosity (Table S3) did not achieve a complete conversion even after 24 h of stirring (Figure S5). Hence, the carbon spheres prepared by hydrothermal carbonization and calcined at low temperature (420 °C) display a greater performance than conventional catalysts prepared with supports such as activated carbon. However, it is important to point out that surface area of supports is not the main feature that influence the catalytic activity. Surface functional groups is the main factor since both XPS and FTIR analyses showed that CN, CCN and CCN-PDA have different profiles of oxygenated groups. These functional groups can prevent Ru leaching from each support surfaces and can affect the catalytic performance during oxidative cleavage tests. Thus a developed surface area along with several oxygen groups (that form complexes with Ru) are required for a good performance in the oxidative cleavage of oleic acid.

The influence of Ru loading was assessed on CCN-PDA supports since the latter displayed the greatest catalytic performance of all tested carbon catalysts. Figure S6 shows that the complete transformation of oleic acid into PA and AA was not possible when Ru loading was decreased to 1 wt% on the carbon support. On the other hand, doubling the Ru loading (i.e. 4 wt%) did not increase neither conversion nor yields and selectivities obtained with CCN-PDA-Ru(2%). In fact, the catalyst with 4 wt% reached 99% of conversion at 7 h which was the same with CCN-PDA-Ru(2%). Therefore, the Ru loading of 2 wt% was maintained for the following of the catalytic assessments.

The stability of the synthesized carbon catalysts was also evaluated by means of recycling tests. Figure 7a shows that CN-Ru(2%) loses catalytic activity after each oxidative cleavage test. The same trend was observed in the case of CCN-Ru(2%) where the conversion after 24 h of agitation diminished down to 72% at the fifth recycle (Figure 7b). On the other hand, the carbon catalyst functionalized with polydopamine maintained its catalytic activity almost intact after five recycling tests (Figure 7c). Only a slight decrease in conversion (about 5%) was registered when CCN-PDA-Ru(2%) was used.

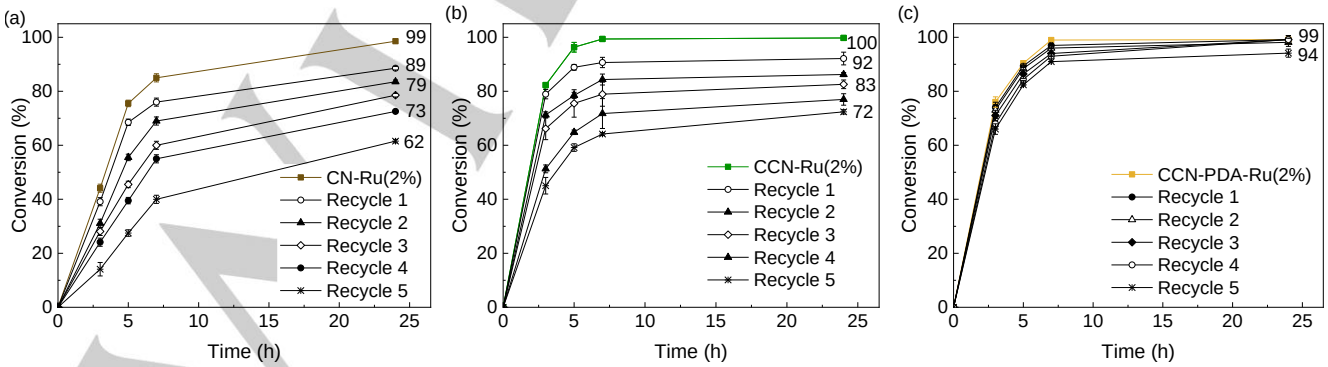


**Figure 7.** Recycling tests of: a) CN-Ru(2%); b) CCN-Ru(2%) and c) CCN-PDA-Ru(2%).

This small drop in catalytic activity can be ascribed to losses of the solid material due to attrition or because of the extensive sampling carried out during the consecutive catalytic tests.

The reason why CN-Ru(2%) and CCN-Ru(2%) lost their catalytic activity after each recycling test is attributed to the leaching of Ru. Since $Ru(VIII)O_4$ is the only species capable of transforming oleic acid into PA and AA, it is believed that a continuous loss of Ru was the main reason for the poor performances of both Ru-carbon catalysts during the last recycling tests. This assumption was confirmed by ICP-AES analyses which showed a reduction of Ru loading on the mentioned solid catalysts after performing the subsequent catalytic tests (Table 4). This was not the case for CCN-PDA-Ru(2%) since the functionalized catalyst with polydopamine maintained almost the same Ru loading as before performing the successive oxidative cleavage runs. From our previous experiences with oxidized carbon black functionalized with PDA, we know that the polymer has the capability to recover Ru ions instead of keeping attached Ru during the whole catalytic test.[47]

**Table 4.** Ru loading on spent carbon catalysts.

| Catalyst | Nominal Ru (wt%)[a] | Superficial Ru (wt%)[b] | Ru loading (wt%)[c] |
|---|---|---|---|
| Spent CN-Ru(2%) | 2.0 | 1.5 | 0.9 |
| Spent CCN-Ru(2%) | 2.0 | 1.8 | 1.1 |
| Spent CCN-PDA-Ru(2%) | 2.0 | 2.1 | 1.7 |

[a] Nominal composition corresponding to 2 wt%. [b] Ru superficial content determined by XPS. [c] Ru loading determined by ICP-AES.

This asseveration was confirmed by Hot-filtration tests (Figure 8) where conversion increased after the extraction of the three different solid catalysts tested in this work. In addition, UV-Visible spectrophotometry analyses from the organic phase showed the presence of $Ru(VIII)O_4$ and $H_2Ru(VI)O_4$ confirming that Ru was detached from the carbon surface (Figure S7). Therefore, it is demonstrated that CCN-PDA-Ru(2%) behaves in the same manner as our previous carbon black-PDA-Ru catalyst. The oxidizing agent transforms the Ru(III)-catecholate complex into $Ru(VIII)O_4$ which reacts in the liquid phase with oleic acid via a pericyclic [3+2] reaction. The UFA evolves into 9,10 dihydroxystearic acid while the Ru species is reduced into $H_2Ru(VI)O_4$. The latter can be re-oxidized by means of $NaIO_4$ to maintain the catalytic cycle. Characterization on CCN-PDA-Ru(2%) surface was performed by XPS spectroscopy at different time intervals of the reaction. $NaIO_4$ reacted with PDA functional groups during the catalytic tests yielding quinones (Figure S8a). At the same time, quinones can form complexes with reduced Ru to recover the active species (i.e. boomerang catalysis).[47]

The driven force involved in Ru recapture can be explained by considering the consumption of $NaIO_4$. Results in Figure S8b confirms that $NaIO_4$ is totally consumed after 24 h of agitation when CCN-PDA-Ru(2%) is present in the reactor. Conversely, $NaIO_4$ was still present in the liquid phase when CN-Ru(2%) or CCN-Ru(2%) were used as catalysts. Thus, $NaIO_4$ can still oxidize Ru species in the liquid phase avoiding their recapture by oxygen groups from CN or CCN. On the other hand, in the absence of $NaIO_4$ (the 8 equivalents of $NaIO_4$ are consumed by the oxidation of catechol groups) the resulted quinone groups can form complexes with Ru species acting as a redox ligand. By this way it is possible to maintain almost the same catalytic activity throughout several catalytic tests.

Although carbon particles before and after the calcination treatment possessed a greater amount of oxygenated groups than CCN-PDA, the former supports did not manage to re-incorporate Ru species as the one with polydopamine did. This shows that a random distribution of several oxygenated functional groups was not enough to re-capture Ru ions once the oxidative cleavage test ended. On the contrary, a periodic distribution of catechol groups within PDA monomers ensured the recovery of Ru species to maintain the catalytic activity of the synthesized catalyst. Hence the real benefit of the polymer is related to its capability to complex Ru through its well organized functional groups.

**Influence of NMO in the oxidative cleavage reaction**

CCN-PDA-Ru(2%) was selected to verify the influence of N-methylmorpholine N-oxide (NMO) as a green oxidizing agent in the oxidative cleavage of oleic acid. When $NaIO_4$ was completely replaced by NMO no catalytic activity was detected at all (Figure 9a). The reason is related to NMO capacity to only regenerate $H_2Ru(VI)O_4$ into $Ru(VIII)O_4$ as is depicted in Figure S9. This means that NMO cannot oxidize the Ru(III)-catecholate complex on CCN surface to transform it into the Ru active species.

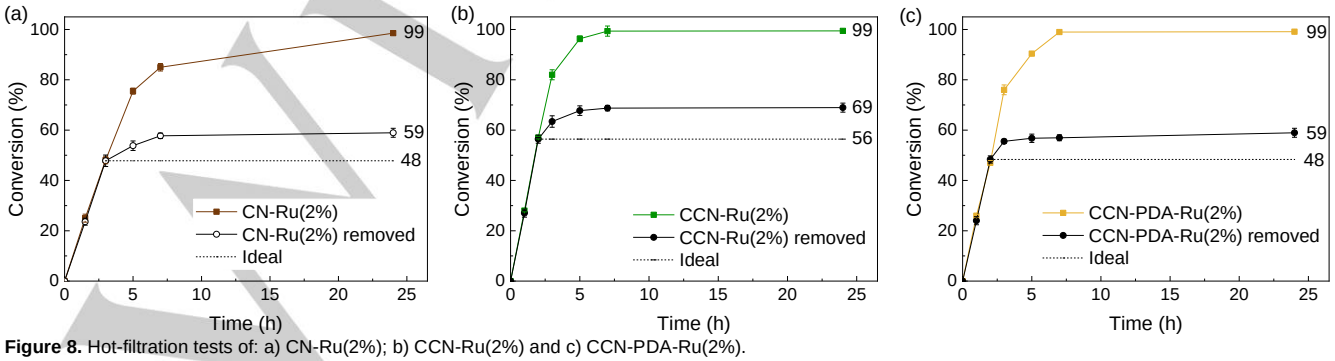


**Figure 8.** Hot-filtration tests of: a) CN-Ru(2%); b) CCN-Ru(2%) and c) CCN-PDA-Ru(2%).

As a consequence, the oxidative cleavage reaction does not take place with only NMO. This fact was confirmed during UV-visible analyses (Figure S10) where $Ru(VIII)O_4$ was not produced after the addition of NMO in the reaction medium. Hence, it is not possible to completely replace sodium periodate as the main oxidizing agent in the oxidative cleavage reaction with our Ru-carbon catalysts.

When 4 equivalents of NMO were combined with 4 equivalents of $NaIO_4$, the catalytic activity was greater than with 8 equivalents of sodium periodate. Actually, with the NMO/$NaIO_4$ combination the greatest catalytic activity was achieved which led to a total conversion after 5 h of reaction. To understand these results it is necessary to keep in mind at what stages of the oxidative cleavage reaction the oxidizing agent can intervene. According to the pathway already explained and detailed in our previous publication[47], the oxidizing agent reacts with: 1) the Ru(III)-catecholate complex on the carbon support surface for its transformation into $Ru(VIII)O_4$; 2) in the liquid phase, it can also take part in the oxidation of $H_2Ru(VI)O_4$ into $Ru(VIII)O_4$ to maintain the catalytic activity of Ru in the oxidative cleavage of UFAs; and 3) it can also intervene in the oxidation of nonanal and 9-oxononanoic acid towards pelargonic and azelaic acids. It was already demonstrated that NMO cannot transform the Ru(III)-catecholate complex into $Ru(VIII)O_4$ while it is well known from the literature the ability of NMO to re-oxidize Ru(VI) species into $Ru(VIII)O_4$.[39,40]

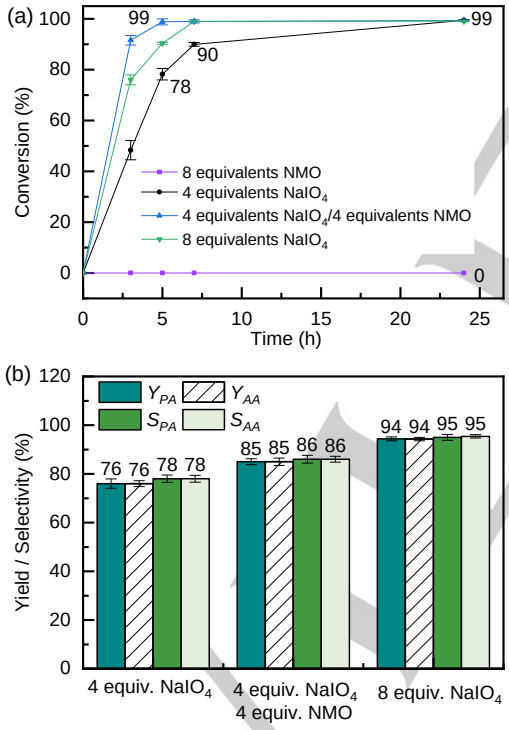


**Figure 9.** a) Catalytic activity of CCN-PDA-Ru(2%) in the oxidative cleavage of oleic acid with different combinations of oxidizing agents. b) Yields and selectivity achieved with different combinations of oxidizing agents.

Then, to verify if NMO can transform oxidative cleavage intermediates into carboxylic acids, nonanal oxidation was carried out with this amine oxide. Nevertheless, NMO cannot perform the oxidation of nonanal into pelargonic acid either (Figure S11). Hence, NMO is only useful for the re-oxidation of reduced Ru(VI) species into $Ru(VIII)O_4$ which is the active species responsible for the transformation of oleic acid into 9,10 dihydroxystearic acid.

Based on these results and explanations, it is possible to affirm that there is a synergistic effect when NMO and $NaIO_4$ are used in equal amounts. While $NaIO_4$ can intervene in the oxidation of the Ru(III)-catecholate complex on CCN surface as well as the oxidation of nonanal and 9-oxononaoic acid into PA and AA, NMO can focus in the re-oxidation of the Ru(VI) active species to improve the catalytic activity during the oxidative cleavage reaction. On the contrary, $NaIO_4$ by itself is distributed among the abovementioned stages of the oxidative cleavage reaction. Thus, with less $NaIO_4$ (i.e. 4 equivalents) the production of PA and AA is not complete as observed in Figure 9b, and only with a greater amount of this oxidizing agent (i.e. 8 equivalents), yields and selectivity of both oxidative cleavage products are almost complete.

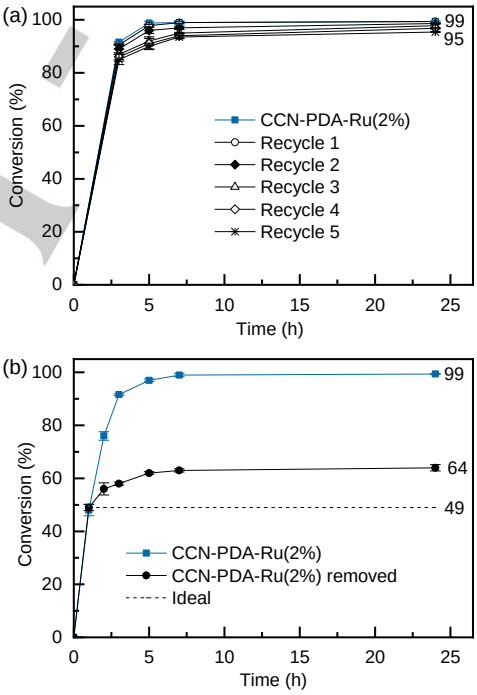


**Figure 10.** a) Recycling tests with CCN-PDA-Ru(2%) along with 4 equiv. $NaIO_4$/4 equiv. NMO; b) Hot-filtration test with CCN-PDA-Ru(2%) along with 4 equiv. $NaIO_4$/4 equiv. NMO.

Although NMO mixed with $NaIO_4$ completely transformed oleic acid within 5 h of stirring, yields and selectivity of PA and AA were 10% lower than the test with 8 equivalents of $NaIO_4$. This reduction in selectivity is ascribed to the lesser amount of $NaIO_4$ and the inability of NMO to oxidize intermediates into the desired oxidative cleavage products. Nevertheless, with the addition of NMO, it was possible to diminish the excess of $NaIO_4$ (which has

detrimental effects on the environment) without ostensibly sacrificing the catalytic activity of the designed carbon catalyst.

Finally, recycling tests were carried out using 4 equivalents of $NaIO_4$ mixed with 4 equivalents of NMO in the reaction medium. Figure 10a shows that CCN-PDA-Ru(2%) catalyst was still active even after 5 consecutive catalytic tests as when 8 equivalents of $NaIO_4$ was used. The Hot-filtration test (Figure 10b) confirmed the presence of Ru species in the reaction medium due to the increase of conversion after the removal of the solid catalyst. In the same way as with $NaIO_4$, the functionalized support can recapture Ru species from the liquid phase and maintain the catalytic activity of the solid catalyst. Hence, the addition of NMO was not an impediment for polydopamine functional groups capability to recover Ru species from the reaction medium.

## Conclusion

Hydrothermal carbonization of an aqueous glucose solution led to the production of very regular carbon spheres which possess a great number of different functional groups *a priori* suitable for transition metals complexation. TEM analyses confirmed the spherical shape of the as synthesized carbon particles while Boehm's titration determined the total acidity of this carbon support. By means of this simple and eco-friendly methodology, it was possible to generate several oxygenated groups on carbon nanoparticles surface in a greater amount than with other dangerous and polluting procedures such as oxidations with $HNO_3$ or $KMnO_4/H_2O_2$. Hence, hydrothermal carbonization is a green alternative for the development of new carbon supports suitable for various applications including catalysis.

The post-calcination treatment was beneficial for the reduction of carbon particles size and for the increase of their specific surface area. The oxygen inside the oven reacted with the outer layers of the carbon particles producing $CO_2$. The latter in turn reacts with carbon atoms on the outer surface producing CO and oxygenated groups. The loss of carbon atoms during this gasification process led to the creation of porosity (mostly micropores) which increases the specific surface area of the support. This aspect was verified by $N_2$ physisorption which confirmed that CCNs possessed a type I isotherm characteristic of microporous materials with pores sizes from 1.0-1.5 nm. Our work thus demonstrates that it was possible to modify the textural properties of carbon spheres through a simple calcination treatment in a short period of time (i.e. 20 minutes).

After the impregnation of Ru on carbon particles with and without calcination, the oxidative cleavage reaction of oleic acid was carried out. The catalytic tests demonstrated that the textural properties of the carbon support have an important impact in the catalytic activity of the as prepared solid catalysts. Although in our previous publication it was demonstrated that the reaction is mostly carried out in the liquid phase, the results reported in this article confirm that a carbon material with higher surface area possessed a greater catalytic activity than a macroporous/non porous material. This was determined that the textural properties of the support play an important role in the oxidative cleavage of UFAs.

The deposition of polydopamine on calcined carbon particles surface was demonstrated by FTIR, TGA and XPS analyses. The real benefit of the polymer coating was observed during the oxidative cleavage tests. After performing 5 recycling tests, the functionalized catalyst maintained its catalytic activity almost intact. Although Ru species were dissolved in the reaction medium, functional groups of polydopamine manage and re-adsorb Ru to regenerate the solid catalyst. By this way, the CCN-PDA-Ru(2%) catalyst remained active up to five catalytic tests with great yields and selectivity towards pelargonic and azelaic acids.

Finally, the possibility to completely replace $NaIO_4$ as oxidizing agent in the oxidative cleavage reaction by N-Methylmorpholine N-oxide (NMO) was explored. The latter is a green oxidant which is active in the re-oxidation of $H_2Ru(VI)O_4$ into $Ru(VIII)O_4$ species. Although it was not possible to perform the oxidative cleavage reaction with only NMO, a combination of $NaIO_4$ and NMO (4 equiv./4 equiv.) increased the catalytic activity of CCN-PDA-Ru(2%) by reducing the reaction time needed to achieve complete conversion. While NMO focused in the re-oxidation of Ru species, $NaIO_4$ can intervene at other stages of the oxidative cleavage reaction (i.e. oxidation of the Ru(III)-catecholate complex as well as the intermediates). Hence, the synergistic effect of the $NaIO_4$/NMO combination allowed to reduce the excess of $NaIO_4$ (which is detrimental for the environment) used in previous catalytic tests without losing the catalytic activity in the oxidative cleavage of oleic acid.

## Experimental Section

**Synthesis of carbon submicrometric particles by hydrothermal carbonization**

In a typical procedure, 100 mL of a 0.2 mol/L D(+)-glucose ($C_6H_{12}O_6$, >98% anhydrous from Carl Roth) solution was prepared and introduced in a 120 mL Teflon lined stainless steel autoclave. The latter was sealed and heated inside an electric MEMMERT GmbH oven at 180 °C for 24 hours. Carbon particles (CNs) were recovered by vacuum filtration using Whatman® PTFE membrane filters (diameter 47 mm, pore size = 0.22 µm) after the autoclave reached the room temperature. All organic residues were removed from CNs through several washings with warm distilled water (~80 °C) and ethanol ($C_2H_6O$, 95% from VWR) until the recovered solution was colorless. Next, CNs were dried at 100 °C for three hours followed by a calcination stage under air in a Vecstar furnace already preheated at 420 °C for 20 minutes in order to produce calcined carbon particles (CCNs).

**Polydopamine deposition on calcined carbon particles**

First, 100 mL of a 10 mM tris(hydroxymethyl)aminomethane (TRIS, $C_4H_{11}NO_3$, >99.0% from TCI chemicals) solution was prepared to obtain a buffer solution at pH = 8.5. Then 110 mg (amount of dopamine from calculations using measures in Figure S2) of dopamine hydrochloride ($C_8H_{11}NO_2$, >98% from TCI chemicals) was dissolved in the TRIS solution which was magnetically stirred for 15 minutes under air atmosphere. After the transparent solution became pale brown (i.e. polymerization of dopamine begins), 1 g of dried CCNs was introduced in the reactor. The suspension was magnetically agitated for 24 h under air atmosphere at room temperature to promote a complete deposition of the polymer on the support. Afterwards, the modified carbon particles, denoted from now on as CCN-PDA, were recovered through centrifugation at 14 000 rpm (26 200 g) in a Heraeus MultifugeX1R

Centrifuge for 40 minutes. Finally, the functionalized support was washed with distilled water and dried overnight under air atmosphere at room temperature.

### Catalysts preparation

Ruthenium(III) chloride hydrate, 99.9% (PGM basis), ($RuCl_3.H_2O$, Ru 38%) from Alfa Aesar was employed for catalysts preparation. Prior Ru impregnation on 500 mg of activated carbon (ACO), CNs, CCNs and CCN-PDA, the mentioned supports were submitted to ultrasound treatment inside 20 mL of distilled water for 15 minutes. Then, 10 mL of a $RuCl_3.H_2O$ solution (10 mM) was added to the suspension of each carbon support in order to attain a Ru load of 2 wt% (Scheme 1). The suspensions were magnetically stirred for 24 h before the catalyst was separated from the solution by centrifugation at 14 000 rpm (26 200 g) in a Heraeus MultifugeX1R Centrifuge. In addition, the synthesized catalysts were washed with distilled water and dried in air ambient at room temperature. From now on the catalyst synthesized with CNs and CCNs are denoted as CN-Ru(2%) and CCN-Ru(2%) respectively. The carbon support functionalized with polydopamine and Ru is named as CCN-PDA-Ru(2%).

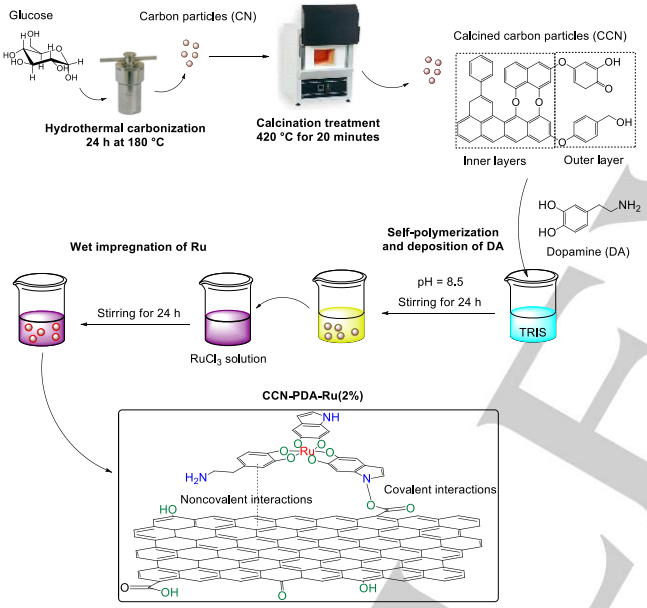


**Scheme 1.** Carbon particles synthesized by hydrothermal carbonization followed by a calcination treatment and functionalized with PDA and Ru.

### Characterization

The morphology of the synthesized carbon materials was assessed through transmission electron microscopy (TEM) in a LEO 922 microscope with an acceleration voltage of 200 kV and equipped with a LaB6 thermal cathode. In addition, the diameter of 20-25 spheres from each carbon material was measured to build a frequency distribution histogram with the aim to determine the mean particle size of each sample. Textural properties of carbon particles were evaluated through $N_2$ physisorption at -196 °C in a Micromeritics Tristar 3000 equipment. About 60 mg of each sample was degassed for 12 h under vacuum (~10.7 Pa) at 150 °C. The Brunauer-Emmet-Teller (BET) method was employed to measure the total surface area using the adsorption isotherm in the partial pressure (P/Po) range from 0.05 to 0.30. As regards microporous carbon materials, a lower P/Po range from 0.004 to 0.08 was employed for the BET method application.[48] In addition, the t-plot method was used to estimate the external surface area by the slope of the line drawn in the linear portion of 0.3 < P/Po < 0.8. The micropore volume was determined after multiplying the intercept of the t-plot (in mol/g) by the density conversion factor = 34.53496 $cm^3$/mol. Then, micropore specific surface area was estimated after calculating the difference between the total surface area and the external surface area while the total pore volume was measured at P/Po = 0.98. Pore size distribution was estimated by Barrett, Joyner and Halenda method (BJH) using the data from the desorption isotherm branch.[48,49] For microporous materials the micropore volume was estimated with the Dubinin-Radushkevich (DB) method in a P/Po < 0.1 range whereas micropore size distribution was estimated by means of the Horvath-Kawazoe (HK) method.[50,51] The thermal stability of carbon materials was evaluated by means of thermogravimetric analysis (TGA). About 2 mg of each sample was introduced into 70 µL $Al_2O_3$ crucibles and submitted under $N_2$ atmosphere from 50 °C to 900 °C in a Mettler Toledo TGA/SDTA851e Thermogravimetric Analyzer. The heating ramp was kept at 10 °C/min and the $N_2$ flow rate was adjusted to 40 mL/min. In addition, the amount of PDA deposited on CCNs surface was calculated by subtracting the weight loss of CCN-PDA from the weight loss of CCNs.

Chemical characterization of carbon particles was performed by Fourier transform infrared spectroscopy (FTIR). In a typical analysis 15 mg of sample was mixed with 300 mg of potassium bromide (KBr, >99% from Acros Organics) dried overnight at 110 °C. Wafers were prepared after compacting the samples in a press. Samples were analyzed in a Bruker Equinox 55 FTIR spectrometer in transmission mode. FTIR spectra were recorded after performing 100 scans in the range of 4000 to 400 $cm^{-1}$ with 4 $cm^{-1}$ of resolution. In addition, Boehm's titration was conducted to quantify the amount of oxygenated groups on all synthesized carbons supports. For each carbon material, three samples of 0.5 g were added to three 50 mL solutions of 0.05 M NaOH, $Na_2CO_3$ and $NaHCO_3$ (reagent grade from Sigma-Aldrich). After degassing all suspensions for 1 h, they were magnetically stirred for 23 h under argon atmosphere. On one hand, the solids were separated by vacuum filtration with the aid of a filter paper (pore size: 0.2 µm). On the other, 10 mL of each filtered solution was acidified with 20 mL of a 0.05 M HCl (37 v/v% from Sigma-aldrich) solution. The new solutions were agitated and continuously degassed for 2 hours under argon atmosphere. Afterwards, all samples were titrated with a 0.05 M NaOH solution using phenolphthalein as indicator.[52] The three basic solutions allow to measure different oxygenated groups on carbon surfaces. Precisely, NaOH neutralizes all acidic functional groups (i.e. phenols, lactones and carboxylic acids) while $Na_2CO_3$ neutralizes lactones and carboxylic groups. Finally, $NaHCO_3$ neutralizes only carboxylic groups so by subtracting the results obtained with each base, the amount of phenols, lactones and carboxylic groups on each carbon material were estimated.[52,53]

Ru loading on each carbon catalyst was determined through ICP-AES spectrophotometry in a ICP 6500 Thermo Scientific Instrument. About 100 mg of each carbon material was calcined under air in a Vecstar furnace already preheated at 550 °C. Then, 1g of NaOH and $Na_2O_2$ (97% from Sigma-Aldrich) were added to the calcined samples melted on the flame of a Bunsen burner. ICP analyses were conducted after 1000 mL of a 10 v/v% HCl solution dissolved the melted samples. The chemical environment of Ru as well as its oxidation state was verified by X-ray photoelectron spectroscopy (XPS). The analyses were performed in a SSX 100/206 photoelectron spectrometer from Surface Science Instruments (USA) equipped with a monochromatized micro focused Al X-ray source (powered at 20 mA and 10 kV). For this purpose, 10 mg of each sample was pressed in small stainless steel troughs with 4 mm diameter. Then, all samples were placed on a ceramic carousel covered with a Ni grid required for charge stabilization. Samples inside the carousel were degassed in a vacuum chamber ($10^{-7}$ Pa) overnight. Then, samples were transferred to the analysis chamber ($10^{-9}$ Pa) to start the analyses. The flood gun was set at 8 eV while the angle between the surface and the axis of the analyzer lens was set at 55°. The analyzed area was ~1.4 $mm^2$ with a pass energy of 150 eV. The full width measured at half maximum (FWHM) of the Au $4f_{7/2}$ peak for a clean gold standard sample was about 1.6 eV. For each sample, the following sequence of spectra was recorded: survey spectrum, C 1s, O 1s, N 1s,

Cl 2p and Ru 3p. In addition, an additional C 1s spectrum was recorded to check the stability of charge compensation with time. Calibration of the binding energy scale was performed by fitting the C1s peak at 284.8 eV. The CasaXPS program (Casa Software Ltd, UK) was employed for the data treatment. The Ru 3p core level was used for the identification and quantification of Ru in order to avoid overlapping issues of C 1s and Ru 3d peaks.[54]

#### Catalytic tests

All tests were carried out by adding 0.5 mmol of oleic acid (OA, $C_{18}H_{34}O_2$, >99.9% GC from TCI chemicals) into a solvent mixture of $H_2O$/MeCN/AcOEt (4/2/1) (MeCN, $C_2H_3N$ >99.98% GC and ethyl acetate (AcOEt, $C_4H_8O_2$ > 99.9% GC from Carl Roth) along with 8 equivalents of sodium periodate ($NaIO_4$, >99% from Sigma-aldrich) and heptanoic acid as internal standard (IS, $C_7H_{14}O_2$, >98% GC from TCI chemicals). Afterwards, 100 mg of catalyst was introduced in the reactor and the suspension was magnetically stirred at 1500 rpm for 24 h at room temperature. The influence of 4-Methylmorpholine N-oxide monohydrate (NMO, $C_5H_{11}NO_2.H_2O$, 98+% from Alfa Aesar) was also evaluated by adding a mixture of 4 equivalents of $NaIO_4$ and 4 equivalents of NMO. The monitoring of the reaction was conducted by injecting 1.5 mL samples (0.1 mL organic layer + 1.4 mL of AcOEt) in a Varian 3800 Gas Chromatograph equipped with a Flame Ionization Detector (FID) and a Stabilwax-DA Restek column (crossbond acid-deactivated Carbowax polyethylene glycol). The procedure of conversion and yields calculation is detailed in the supporting information. It is important to mention that three subsequent extractions from the aqueous phase were conducted after a catalytic test ended. These extractions were conducted with 2 mL of fresh AcOEt in order to recover all the pelargonic (PA) and azelaic acid (AA) that could have formed an emulsion.

The oxidative cleavage of oleic acid was monitored by UV-Vis spectrophotometry in a UV-3600 Plus Shimadzu spectrophotometer equipped with a deuterium lamp (light source for the ultraviolet range) and a WI halogen lamp (light source for the visible and near infrared range). Samples from organic phase were extracted separately at different time intervals and placed in quartz cells to be analized by UV-Visible spectroscopy in absorbance configuration. The idea was to verify the presence of Ru species during the reaction and after it was completed. In addition, the consumption of $NaIO_4$ was determined by measuring the absorbance of the peak at 222 nm corresponding to the oxidizing agent.[55] All tests were carried out from 600 to 200 nm range and spectra were recorded with a resolution of 0.5 nm.

Recycling tests were conducted to verify the catalytic stability of the carbon catalysts. The recovered catalyst was thoroughly washed with warm distilled water (~80 °C) and dried overnight under air atmosphere at room temperature. Then, it was re-incorporated in a fresh reaction mixture to start again a new oxidative cleavage test. Five recycling tests were conducted to evaluate the same catalytic activity remained or not. In addition, hot-filtration tests were performed to verify if the reaction is taking place on catalysts surface. When conversion during a catalytic test arrived around 50%, the carbon catalyst was removed from the reaction medium by centrifugation in a Heraeus MultifugeX1R Centrifuge at 14 000 rpm (26 200 g) for 30 minutes. The stirring of the reaction mixture continued up to 24 h with sampling at different time intervals. The purpose of this procedure was related to verify if an increase in conversion after the catalyst removal was observed. The latter would suggest that Ru has moved into the liquid phase diminishing the catalytic performance of the carbon catalysts in subsequent catalytic tests.

## Acknowledgements

The authors want to thank the “Université catholique de Louvain” for the scholarship granted to Sebastián Gámez in the frame of the “Coopération au développement” doctoral program.

## Conflicts of interest

There are no conflicts to declare.

**Keywords:** Carbon particles • Heterogeneous catalysis • Oleic acid • Oxidative cleavage • Polydopamine

[1] A. Enferadi Kerenkan, F. Béland, T. O. Do, *Catal. Sci. Technol*. **2016**, 6, 971–987. https://doi.org/10.1039/c5cy01118c.
[2] C. Aranda, A. Olmedo, J. Kiebist, K. Scheibner, J. C. del Río, A. T. Martínez, and A. Gutiérrez, *ChemCatChem*. **2018**, 10, 3964–3968. https://doi.org/10.1002/cctc.201800849.
[3] A. Corma Canos, S. Iborra, A. Velty, *Chem. Rev*. **2007**, 107, 2411–2502. https://doi.org/10.1021/cr050989d.
[4] M. Mittelbach, *Eur. J. Lipid Sci. Technol*. **2015**, 117, 1832–1846. https://doi.org/10.1002/ejlt.201500125.
[5] U. Biermann, U. Bornscheuer, M. A. R. Meier, J. O. Metzger, H. J. Schäfer, *Angew. Chem. Int. Ed*. **2011**, 50, 3854–3871. https://doi.org/10.1002/anie.201002767.
[6] W. Zhang, J. Lee, S. Younes, F. Tonin, P. Hagedoorn, H. Pichler, Y. Baeg, J. Park, R. Kourist, F. Hollmann, *Nat Commun*. **2020,** 2258. https://doi.org/10.1038/s41467-020-16099-7.
[7] D. Yun, Z. Zhang, D. W. Flaherty, *React. Chem. Eng*. **2022**, 7, 2054-2065. https://doi.org/10.1039/D2RE00160H.
[8] A. Vassoi, T. Tabanelli, A. Sacchetti, F. Di Gioia, L. Capuzzi, and F. Cavani, *ChemSusChem*. **2021**, 14, 2375–2382. https://doi.org/10.1021/ol1023807.
[9] N. Obara, S. Hirasawa, M. Tamura, Y. Nakagawa, K. Tomishige, *ChemCatChem*. **2016**, 8, 1732–1738. https://doi.org/10.1002/cctc.201600153.
[10] J. S. Yu, A. K. Kim, *J Biomed Sci*. **2010**, 17, S45. https://doi.org/10.1186/1423-0127-17-S1-S45.
[11] R. Ciriminna, A. Fidalgo, L. M. Ilharco, M. Pagliaro, *Biofuels, Bioprod. Biorefin*. **2019**, 13, 1476–1482. https://doi.org/10.1002/bbb.2046.
[12] C. A. Hone, A. O’Kearney-McMullan, R. Munday, C. O. Kappe, *ChemCatChem*. **2017**, 9, 3298–3302. https://doi.org/10.1002/cctc.201700671.
[13] K. B. Otte, J. Kittelberger, M. Kirtz, B. M. Nestl, B. Hauer. *ChemCatChem*. **2014**, 6, 897–897. https://doi.org/10.1002/cctc.201490020.
[14] A. Soutelo-Maria, J. L. Dubois, J. L. Couturier, G. Cravotto, *Catalysts* **2018**, 8, 464. https://doi.org/10.3390/catal8100464.
[15] J. Vondran, M. Peters, A. Schnettger, C. Sichelschmidt, T. Seidensticker, *Catal. Sci. Technol*. **2022**, 12, 3622-3633. https://doi.org/10.1039/D1CY02317A.
[16] R. Schlögl, Heterogeneous catalysis. *Angew. Chem. Int. Ed*. **2015**, Wiley-VCH Verlag. https://doi.org/10.1002/anie.201410738.
[17] F. Papafotiou, K. Karidi, A. Garoufis, M. Louloudi,. *Polyhedron*. **2013**, 52, 634–638. https://doi.org/10.1016/j.poly.2012.07.094.
[18] L. Leckie, S. F. Mapolie, *Appl. Catal., A*. **2018**, 565, 76–86. https://doi.org/10.1016/j.apcata.2018.07.038.
[19] M. Sevilla, A. B. Fuertes, *Carbon*. **2009**, 47, 2281–2289. https://doi.org/10.1016/j.carbon.2009.04.026.
[20] M. H. Joula, M. Farbod, *Appl. Surf. Sci*. **2015**, 347, 535–540. https://doi.org/10.1016/j.apsusc.2015.04.118.
[21] G. Ischia, M. Cutillo, G. Guella, N. Bazzanella, M. Cazzanelli, M. Orlandi, A. Miotello, L. Fiori, *Chem. Eng. J*. **2022**, 449, 137827. https://doi.org/10.1016/j.cej.2022.137827.

[22] Y. Ogihara, R. L. Smith, H. Inomata, K. Arai, Cellulose. 12, 595–606 (2005). https://doi.org/10.1007/s10570-005-9008-1.

[23] H. Simsir, N. Eltugral, S. Karagoz, *Energy Fuels*. **2019**, 33, 7473-7479. https://doi.org/10.1021/acs.energyfuels.9b01750.

[24] N. Shi, Q. Liu, Y. Liu, L. Chen, N. Chen, J. Peng, L. Ma, *Energy Fuels.* **2020**, 34, 1830–1840. https://doi.org/10.1021/acs.energyfuels.9b03747.

[25] Q. He, Y. Yu, J. Wang, X. Suo, Y. Liu, *Ind. Eng. Chem. Res*. **2021**, 60, 12, 4552–4561. https://doi.org/10.1021/acs.iecr.0c06280.

[26] X. Li, K. Peng, Q. Xia, X. Liu, Y. Wang, *Chem. Eng. J*. **2018**, 332, 528–536, https://doi.org/10.1016/j.cej.2017.06.105.

[27] T. M. Aida, Y. Sato, M. Watanabe, K. Tajima, T. Nonaka, H. Hattori, K. Arai, *J. Supercrit. Fluids*. **2007**, 40, 381–388. https://doi.org/10.1016/j.supflu.2006.07.027.

[28] T. A. Khan, A. S. Saud, S. S. Jamari, M. H. A. Rahim, J. W. Park, H. J. Kim, *Biomass and Bioenergy*. **2019**, 130, 105384. https://doi.org/10.1016/j.biombioe.2019.105384.

[29] A. Chacón-Parra, P. van Eyk, *Fuel*. **2022**, 309, 122169. https://doi.org/10.1016/j.fuel.2021.122169.

[30] F. S. Asghari, H. Yoshida, *Ind. Eng. Chem. Res*. **2006**, 45, 7, 2163–2173. https://doi.org/10.1021/ie051088y.

[31] C. Falco, N. Baccile, M. M. Titirici, *Green Chem*. **2011**, 13, 3273–3281. https://doi.org/10.1039/C1GC15742F.

[32] A. Jain, R. Balasubramanian, M. P. Srinivasan, *Chem. Eng. J*. **2016**, 283, 789–805. https://doi.org/10.1016/j.cej.2015.08.014.

[33] T. Evcil, H. Simsir, S. Ucar, K. Tekin, S. Karagoz, *Fuel*. **2020**, 279, 118458, https://doi.org/10.1016/j.fuel.2020.118458.

[34] M. S. Reza, C. S. Yun, S. Afroze, N. Radenahmad, M. S. Abu Bakar, R. Saidur, J. Taweekun, A. K. Azad, *Arab Journal of Basic and Applied Sciences*. **2020**, 27, 208–238. https://doi.org/10.1080/25765299.2020.1766799.

[35] J. Pallarés, A. González-Cencerrado, I. Arauzo, *Biomass Bioenergy*. **2018**, 115, 64–73. https://doi.org/10.1016/j.biombioe.2018.04.015.

[36] K. Sadamoto, Y. Yamagiwa, H. Sakaki, M. Kurata, *J. Vet. Med. Sci*. **2018**, 80, 901–908. https://doi.org/10.1292/jvms.17-0613.

[37] E. M. Lent, L. C. B. Crouse, W. S. Eck, *Regul. Toxicol. Pharmacol*. **2017**, 83, 23–37. https://doi.org/10.1016/j.yrtph.2016.11.014.

[38] H. Chanzy, S. Nawrot, A. Peguy, P. Smith, J. Chevalier, *J. Polym Sci Polym Phys Ed.* **1982**, 20, 1909–1924. https://doi.org/10.1002/pol.1982.180201014.

[39] B. Balagam, R. Mitra, D. E. Richardson, *Tetrahedron Lett*. **2008**, 49, 1071–1075. https://doi.org/10.1016/j.tetlet.2007.11.186.

[40] K. S. Coleman, L. J. L. Bedel, J. A. Osborn, *Comptes Rendus de l'Academie des Sciences - Series IIc: Chemistry*. **2000**, 3, 765–769. https://doi.org/10.1016/S1387-1609(00)01201-9.

[41] C. Sinha, *Curr. Organocatal*. **2019**, 6, 139–157. https://doi.org/10.2174/2213337206666190311130604.

[42] C. Jiang, G. A. Yakaboylu, T. Yumak, J. W. Zondlo, E. M. Sabolsky, J. Wang, *Renewable Energy*. **2020**, 155, 38–52. https://doi.org/10.1016/j.renene.2020.03.111

[43] De la Torre Chauvin, Ernesto Hale. Préparation de charbon actif à partir de coques de noix de palmier à huile pour la récupération d´or et le traitement d´effluents cyanurés. Supervisors: Gaigneaux, Eric; Lucion, Christian. List of publications and communications, **2015**. http://hdl.handle.net/2078.1/155680.

[44] Shurvell, H. F. In Handbook of Vibrational Spectroscopy. John Wiley & Sons, Ltd, **2006**. https://doi.org/10.1002/0470027320.s4101.

[45] R. Gu, W. Z. Xu, P. A. Charpentier, *J. Polym. Sci., Part A: Polym. Chem*. **2013**, 51, 3941–3949. https://doi.org/10.1002/pola.26802.

[46] Y. Yu, J. G. Shapter, R. Popelka-Filcoff, J. W. Bennett, A. V. Ellis, *J. Hazard. Mater*. **2014**, 273, 174–182. https://doi.org/10.1016/j.jhazmat.2014.03.048.

[47] S. Gámez, E. de la Torre, E. M. Gaigneaux, *Chem. Eng. J*. **2022**, 427, 131820. https://doi.org/10.1016/j.cej.2021.131820.

[48] J. Rouquerol, P. Llewellyn, F. Rouquerol, *Stud. Surf. Sci. Catal*. **2007**, 160, 49–56. https://doi.org/10.1016/s0167-2991(07)80008-5.

[49] F. Rouquerol, L. Luciani, *Techniques de l'Ingénieur*. **2003**, P1050, 1–24. http://cat.inist.fr/?aModele=afficheN&cpsidt=16521113.

[50] C. Nguyen, D. D. Do, *Carbon*. **2001**, 39, 1327–1336. https://doi.org/10.1016/S0008-6223(00)00265-7.

[51] G. Horváth, K. Kawazoe, *J. Chem. Eng. Jpn*. **1983**, 16, 470–475. https://doi.org/10.1252/jcej.16.470.

[52] S. L. Goertzen, K. D. Thériault, A. M. Oickle, A. C. Tarasuk, H. A. Andreas, *Carbon*. **2010**, 48, 1252–1261. https://doi.org/10.1016/j.carbon.2009.11.050.

[53] J. P. Chen, S. Wu, *Langmuir*. **2004**, 20, 2233–2242. https://doi.org/10.1021/la0348463.

[54] D. J. Morgan, *Surf. Interface Anal*. **2015**, 47, 1072–1079. https://doi.org/10.1002/sia.5852.

[55] J. Simon, O. Tsetsgee, N. A. Iqbal, J. Sapkota, M. Ristolainen, T. Rosenau, A. Potthast, *Data in Brief*. **2022**, 40, 107757. https://doi.org/10.1016/j.dib.2021.107757.

10.1002/cctc.202201134




## Entry for the Table of Contents

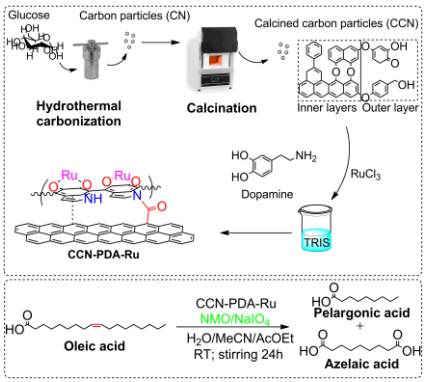


Carbon spheres were synthesized by hydrothermal carbonization of a glucose solution. This carbon support was calcined under air atmosphere to create porosity and functionalized with polydopamine (PDA) to improve their ability to complex Ru ions. The catalyst completed the oxidative cleavage of oleic acid within 7 h of stirring at room temperature with $NaIO_4$ and N-methyl morpholine as oxidizing agents.